

西藏改则蛇绿岩中斜长花岗岩地球化学特征、 锆石 U-Pb 年龄及构造意义

樊帅权^{1,2}, 史仁灯¹, 丁林¹, 刘德亮^{1,2}, 黄启帅^{1,2}, 王厚起^{1,2}

(1. 中国科学院 青藏高原研究所 大陆碰撞与高原隆升重点实验室, 北京 100085;

2. 中国科学院 研究生院, 北京 100049)

摘要: 西藏改则蛇绿岩主要由地幔橄榄岩、均质辉长岩、玄武岩、玄武安山岩和斜长花岗岩组成。其中斜长花岗岩主要由石英、基性斜长石组成, SiO_2 含量较高, 为 72.18% ~ 74.55%, Mg^+ 均值为 42, Na_2O 含量为 1.30% ~ 3.13%, K_2O 含量很低, 为 0.26% ~ 0.67%, $\text{Na}_2\text{O}/\text{K}_2\text{O}$ 变化范围为 3.64 ~ 8.23。斜长花岗岩和中基性岩(辉长岩、玄武岩和玄武安山岩)的元素地球化学特征表明, 改则斜长花岗岩可能是由基性岩部分熔融形成的, 并且斜长花岗岩富集 Sr、Rb 等大离子亲石元素, 亏损 Nb、Ta、Ti 等高场强元素, 具有岛弧型火山岩的特点, 推测该斜长花岗岩形成于岛弧环境, 是 SSZ 型蛇绿岩的组成单元。LA-ICPMS 法测得斜长花岗岩中锆石 U-Pb 加权平均年龄为 189.8 ± 1.9 Ma, 表明班公湖-怒江缝合带改则地区在早侏罗世发生了俯冲作用, 该区的俯冲消减时间要早于西段的班公湖地区, 晚于东段丁青地区。

关键词: 斜长花岗岩; 熔岩; 蛇绿岩; 锆石; 班公湖-怒江缝合带; 构造环境

中图分类号: P588.12; P597⁺.3

文献标识码:A

文章编号: 1000-6524(2010)05-0467-12

Geochemical characteristics and zircon U-Pb age of the plagiogranite in Gaize ophiolite of central Tibet and their tectonic significance

FAN Shuai-quan^{1,2}, SHI Ren-deng¹, DING Lin¹, LIU De-liang^{1,2}, HUANG Qi-shuai^{1,2} and WANG Hou-qi^{1,2}

(1. Key Laboratory of Continental Collision and Plateau Uplift, Institute of Tibetan Plateau Research, Chinese Academy of Sciences, Beijing 100085, China; 2. Graduate University of Chinese Academy of Sciences, Beijing 100049, China)

Abstract: Located in central Tibet, the Gaize ophiolite is a key element within the middle part of the Bangong Co-Nujiang suture zone, marking the boundary between the Lhasa and Qiangtang blocks. It is a tectonic mélange consisting of numerous blocks of mantle peridotite, mafic lavas, isotropic gabbro and plagiogranite, in which, the genesis and tectonic setting of the plagiogranite is important in discussing the evolution of the Bangong Co-Nujiang suture zone. Based on detailed studies of field geological background and petrographical features, the authors selected some samples to analyze the whole-rock content of major elements, trace elements and rare earth elements and determine the ages of zircons separated from the plagiogranite by La-ICP-MS U-Pb method. The results show that the plagiogranite crops out as dykes intruding into gabbro, basalt and basaltic andesite with no thermal aureole along the boundary between the plagiogranite and associated lavas comprising basalt and basaltic andesite. The plagiogranite is mainly composed of quartz and plagioclase with granitice tex-

收稿日期: 2009-12-14; 修訂日期: 2010-05-04

基金项目: 国家自然科学基金面上项目(40972056, 40672051); 中国科学院青藏高原研究所创新项目(07Va081001); 中国地质调查局地调项目(1212010918013)

作者简介: 樊帅权(1985-), 硕士研究生, 构造地质学专业, E-mail: fanshuaiquan@itpcas.ac.cn; 通讯作者: 史仁灯, 副研究员, 从事地幔岩及相关矿产研究, E-mail: shirendeng@itpcas.ac.cn。

ture. The content of SiO_2 is high, varying in the range of 72.18% ~ 74.55% with the $\text{Mg}^{\#}$ of 42, and the content of Na_2O and K_2O is 1.30% ~ 3.13% and 0.26% ~ 0.67%, respectively, with high $\text{Na}_2\text{O}/\text{K}_2\text{O}$ ratios ranging from 3.64 to 8.23. The chondrite normalized REE patterns of the plagiogranite are similar to those of the associated lavas with flat pattern and weak negative anomaly of Eu ($\delta\text{Eu}_N = 0.82 \sim 0.95$). La and Yb versus SiO_2 correlations of the plagiogranite and associated lavas and isotropic gabbro reveal that the plagiogranite resulted from the magma remelting from the associated lavas. Like the associated lavas, the plagiogranite rocks have island arc affinity with HFSE depletion and LILE (Sr, Rb) enrichment, and Nb, Ta and Ti negative anomalies in chondrite-normalized plots indicate that these rocks might have originated in the suprasubduction zone setting. Thus, the plagiogranite and the associated lavas are considered to be members of the SSZ-type ophiolite. The grains of zircons separated from the plagiogranite are about 40 ~ 60 μm in length, with no residual old nuclear and metamorphic edge but the development of banded structure. The values of Th/U between 0.32 and 1.38 (higher than 0.1) suggest that they are magmatic zircons. The average age of zircons in the plagiogranite is 189.8 ± 1.9 Ma, suggesting that the plagiogranite was formed in early Jurassic. The evidence of geochemistry and U-Pb age supports the hypothesis that the subduction occurred at the early Jurassic period in Gaize area within the middle part of the Bangong Co-Nujiang suture zone, earlier than the subduction in the Bangong Co area within the western part of the suture where the activity took place in mid-Jurassic time, but later than the subduction in the Dingqing area within the eastern part of the suture where the activity happened in late Triassic. Combined with previous studies, the authors believe that the Bangong Co-Nujiang Tethys subduction started from east to west during the late Triassic to Jurassic period.

Key words: plagiogranite; lava; ophiolite; zircon; Bangong Co-Nujiang suture; tectonic setting

蛇绿岩是一套可与大洋岩石圈对比的特殊的镁铁-超镁铁质岩石组合,是确定古板块边界的重要证据。依据成因构造背景可将蛇绿岩分为两类:一是形成于洋中脊的MOR型蛇绿岩;另一是形成于俯冲带上的SSZ型蛇绿岩(Pearce *et al.*, 1984; Pearce, 2003)。蛇绿岩中可以含有少量的浅色侵入岩,包括钠长花岗岩、石英闪长岩、更长花岗岩、英云闪长岩和角斑岩,统称为大洋斜长花岗岩。大洋斜长花岗岩是一种 SiO_2 含量高、 Al_2O_3 含量中等、 K_2O 含量低,以浅色矿物石英和长石为主要成分,含有少量铁镁质矿物的岩石,是亚碱性玄武质岩浆在洋中脊这种缓慢扩张的环境中分离结晶形成的(Coleman & Peterman, 1975)。这种斜长花岗岩不仅可在洋中脊环境(MOR)经岩浆分离结晶形成,还可以在俯冲带上(SSZ)由俯冲的洋壳或大洋沉积物部分熔融形成(Pedersen and Malpas, 1984; Sorensen and Grossman, 1989; Flagler and Spray, 1991)。蛇绿岩中这种少量的花岗质岩石是研究蛇绿岩成因和精确定年的重要岩石单元(Coleman & Peterman, 1975)。

班公湖-怒江缝合带是青藏高原上一条重要的

板块边界,研究该带蛇绿岩中斜长花岗岩的成因、构造背景和形成时代,对探讨青藏高原早期构造演化具有重要意义。该带中段改则地区蛇绿岩中存在斜长花岗岩(西藏自治区地质调查院,2002^①;张宽忠等,2007;张玉修等,2007),但是关于其成因及形成时代尚存争议。张宽忠等(2007)对古昌蛇绿岩中斜长花岗岩及其围岩的地球化学特征进行了分析,认为该斜长花岗岩是基性、超基性岩浆分异的残余体或端员岩石,形成于局限洋盆环境。西藏自治区地质调查院(2002)^①认为改则斜长花岗岩是洋脊扩张的产物,源自较深的地幔,是MOR型蛇绿岩的一员,代表晚侏罗世的洋壳,据其全岩K-Ar同位素年龄(124 Ma),推测其于早白垩世时发生构造侵位。张玉修等(2007)认为改则南拉果错蛇绿岩中斜长花岗岩可能为剪切带中含水条件下辉长岩剪切深熔作用形成,其中锆石SHRIMP U-Pb年龄为 166.6 ± 2.5 Ma,推测该区存在中侏罗世洋盆。本文欲通过改则蛇绿岩中斜长花岗岩、伴生熔岩及辉长岩的岩石地球化学特征和锆石U-Pb同位素年龄分析,确定该区蛇绿岩的成因构造背景和形成时代,进而探讨班公

^① 西藏自治区地质调查院. 2002. 中华人民共和国区域地质调查报告改则幅.

湖-怒江缝合带构造演化。

1 地质概况

改则蛇绿岩分布在改则县南约30 km的拉果错一带,总体呈东西向展布,南缘、北缘皆与下白垩统郎山组灰岩呈断层接触。研究区内出露的岩石组合包括橄榄岩、辉长岩、玄武岩、玄武安山岩及斜长花岗岩等(图1),由于受到强烈的构造作用岩石严重破碎,不同组成单元之间均以断层接触,以构造岩块形式产出。蛇绿岩剖面南侧的辉长岩逆冲推覆在郎山组灰岩之上,断层倾向向南。紧邻辉长岩的橄榄岩层底部角砾片理化严重,SC组构指示由北向南的逆冲,片理化角砾层厚约2 m,向北为块状橄榄岩块,角砾成分与块状橄榄岩一致,蛇纹石化严重,仅见副矿物尖晶石新鲜颗粒残留。玄武岩出露在橄榄岩块

北,厚约1500 m,在玄武岩层内部夹杂厚约500 m的碎屑岩。西藏自治区地质调查院区调报告^①通过区域对比,认为这套碎屑岩地层与则弄群相当,因在测区范围出露面积较少,难以进一步划分对比,故引用则弄群一名。碎屑岩与南侧玄武岩以逆冲推覆断层接触,其北侧被玄武岩覆盖,在剖面的北侧被郎山组的灰岩逆冲推覆覆盖。该研究区内,斜长花岗岩在平面上为不规则透镜状,在剖面上呈脉状产出于中部玄武岩中,它们的接触部位未见岩浆侵入的热烘烤现象。

2 岩石学特征

斜长花岗岩呈灰白色,细粒花岗结构,块状构造。矿物粒度为0.2~0.8 mm,主要矿物为石英(45%~55%)和斜长石(40%~45%)。斜长石为半

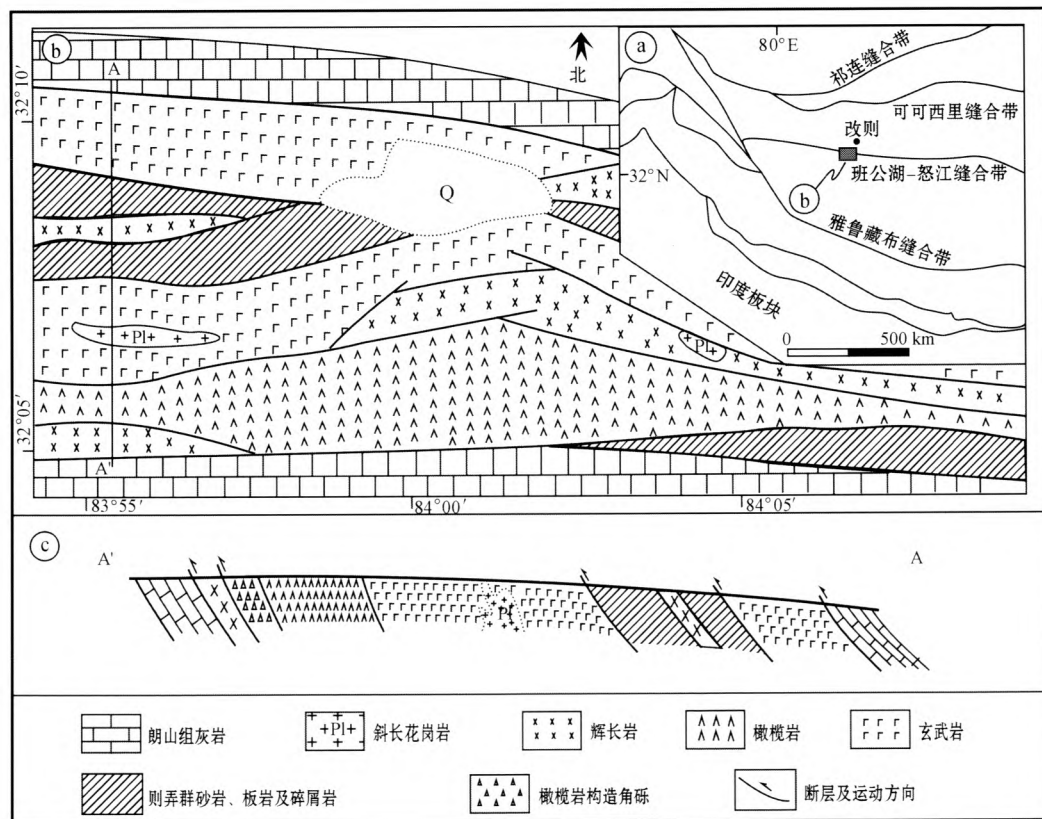


图1 改则蛇绿岩大地构造位置图(a)、蛇绿岩块分布地质简图(b)及采样剖面图(c)

Fig. 1 Schematic map of Gaize ophiolite (a), distribution of ophiolite blocks (b), and geological section of Gaize plagiogranite (c) in northern Tibet

^① 西藏自治区地质调查院. 2002. 中华人民共和国区域地质调查报告改则幅.

自形粒状,聚片双晶不发育,可见简单双晶,无明显的环带构造,因受明显的绢云母化和绿帘石化影响,表面混浊(图2)。石英呈他形粒状生于斜长石晶体之间,局部可见粗大的单晶体。依据全岩化学成分的CIPW计算结果及显微镜下斜长石聚片双晶特点,可知斜长石牌号较高(31~70),平均值为49,属中性斜长石,高于典型的花岗岩中斜长石牌号(10~35)。

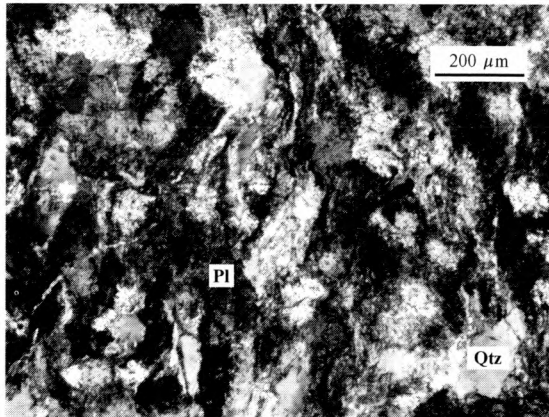


图2 斜长花岗岩样品显微照片(正交偏光)

Fig. 2 Micrographs of plagiogranite
(Pl—斜长石; Qtz—石英)
(Pl—plagioclase; Qtz—quartz)

3 地球化学特征

斜长花岗岩及伴生熔岩的主要元素、稀土元素及微量元素的分析结果见表1。主量元素及Ba、Sr、Zr、Rb在中国地质科学院廊坊物化探研究所采用熔片法-X射线荧光光谱(XRF)和容量法(VOL)完成,微量元素及稀土元素采用ICP-MS法完成。分析结果显示,斜长花岗岩的SiO₂含量较高,变化范围为72.18%~74.55%,K₂O含量非常低,约为0.26%~0.67%,Na₂O+K₂O=1.56%~3.51%,Al₂O₃含量为11.9%~13.22%,CaO含量的变化范围相对较大,为2.49%~6.27%,Mg[#]变化范围为37~52,均值为42。与斜长花岗岩伴生的熔岩在TAS图解(图3)上主要属于玄武岩和玄武安山岩范畴。

斜长花岗岩具轻微的LREE富集(图4)。 $\sum \text{LREE} = 21.87 \times 10^{-6} \sim 29.07 \times 10^{-6}$, $\sum \text{HREE} = 7.59 \times 10^{-6} \sim 11.26 \times 10^{-6}$, LREE/HREE=2.58~2.96。 $(\text{La/Yb})_N = 1.59 \sim 1.81$, $(\text{La/Sm})_N = 2.08 \sim 2.21$, $(\text{Gd/Yb})_N = 0.73 \sim 0.77$, Eu存在很弱的负异常, $\delta \text{Eu}_N = 0.82 \sim 0.95$ 。斜长花岗岩与伴生熔岩的稀土元素配分曲线基本一致。两者稀土元素组成上

的相似性表明斜长花岗岩是蛇绿岩套的组成部分,因稀土元素具有相似的晶体化学性质,在各种造岩作用中常作为一个整体迁移。在球粒陨石标准化微量元素蛛网图(图5)中,斜长花岗岩富集Sr、Rb等大离子亲石元素,亏损Nb、Ta、Ti等高场强元素,具有岛弧型火山岩的特点。

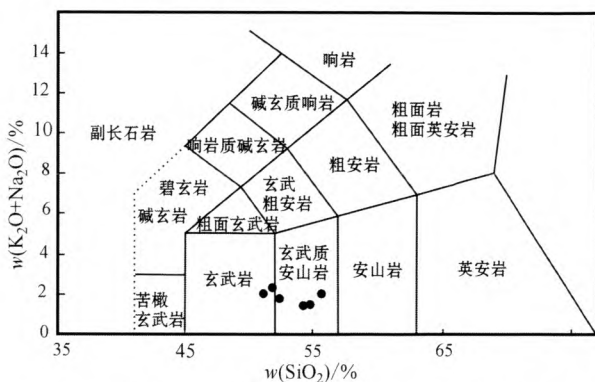


图3 改则蛇绿岩的熔岩 $\text{K}_2\text{O} + \text{Na}_2\text{O} - \text{SiO}_2$ (TAS) 图解
(据 Le Maitre 等, 1989)

Fig. 3 $\text{K}_2\text{O} + \text{Na}_2\text{O} - \text{SiO}_2$ (TAS) diagram of lavas from Gaize ophiolite(after Le Maitre et al., 1989)

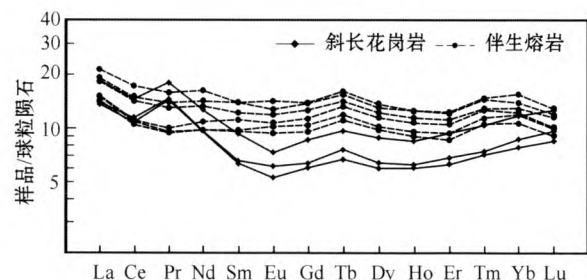


图4 斜长花岗岩及伴生熔岩的球粒陨石标准化稀土元素配分图(标准化数据据 Boynton 等, 1984)

Fig. 4 Chondrite-normalized REE patterns of plagiogranite and associated lavas (after Boynton et al., 1984)

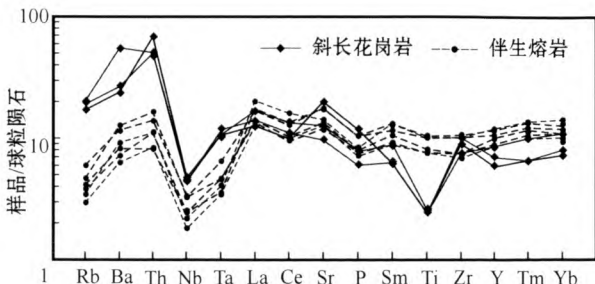


图5 斜长花岗岩及伴生熔岩的球粒陨石标准化微量元素蛛网图(标准化数据据 Thompson 等, 1982)

Fig. 5 Chondrite-normalized trace element spider diagram of plagiogranite and associated lavas (after Thompson et al., 1982)

表1 斜长花岗岩、玄武岩和玄武质安山岩的主量元素($w_B/\%$)和微量元素($w_B/10^{-6}$)分析结果Table 1 Chemical composition ($w_B/\%$) and trace element abundance ($w_B/10^{-6}$) of plagiogranite and basalt

| 样号 | 斜长花岗岩 | | | 玄武安山岩 | | | | 玄武岩 | |
|--------------------------------|--------|--------|--------|--------|--------|--------|--------|--------|--------|
| | 08087A | 08087B | 08087C | 08087D | 08087F | 08087G | 08087H | 08087E | 08087I |
| SiO ₂ | 72.18 | 74.55 | 72.51 | 55.79 | 52.46 | 54.51 | 54.31 | 51.19 | 51.91 |
| TiO ₂ | 0.23 | 0.24 | 0.26 | 1.01 | 0.83 | 1.05 | 1.07 | 0.78 | 0.78 |
| Al ₂ O ₃ | 11.90 | 12.77 | 13.22 | 15.12 | 14.84 | 15.08 | 15.45 | 15.23 | 15.10 |
| Fe ₂ O ₃ | 3.78 | 2.25 | 1.84 | 3.99 | 4.10 | 4.29 | 4.88 | 1.47 | 3.75 |
| FeO | 1.47 | 1.17 | 2.27 | 5.26 | 4.18 | 6.16 | 5.76 | 6.79 | 4.87 |
| MnO | 0.07 | 0.05 | 0.07 | 0.16 | 0.14 | 0.17 | 0.17 | 0.14 | 0.15 |
| MgO | 0.93 | 1.25 | 1.33 | 5.11 | 7.31 | 5.55 | 5.67 | 7.78 | 8.02 |
| CaO | 6.27 | 2.49 | 3.48 | 8.87 | 12.14 | 8.90 | 8.76 | 11.72 | 10.32 |
| Na ₂ O | 1.30 | 3.13 | 2.44 | 2.01 | 1.70 | 1.52 | 1.40 | 2.00 | 2.24 |
| K ₂ O | 0.26 | 0.38 | 0.67 | 0.07 | 0.09 | 0.12 | 0.12 | 0.10 | 0.11 |
| P ₂ O ₅ | 0.04 | 0.05 | 0.05 | 0.09 | 0.07 | 0.09 | 0.10 | 0.07 | 0.06 |
| CO ₂ | 0.00 | 0.00 | 0.00 | 0.36 | 0.91 | 0.27 | 0.33 | 0.80 | 0.33 |
| 烧失量 | 1.35 | 1.46 | 1.48 | 2.30 | 2.17 | 2.31 | 2.39 | 2.18 | 2.04 |
| 总量 | 99.78 | 99.79 | 99.62 | 100.14 | 100.94 | 100.02 | 100.41 | 100.25 | 99.68 |
| La | 4.20 | 4.32 | 5.74 | 6.69 | 4.71 | 5.72 | 5.92 | 4.52 | 4.80 |
| Ce | 8.58 | 9.10 | 11.69 | 13.88 | 8.99 | 11.32 | 11.84 | 8.36 | 8.89 |
| Pr | 1.78 | 1.81 | 2.13 | 1.93 | 1.23 | 1.58 | 1.69 | 1.16 | 1.15 |
| Nd | 5.60 | 5.63 | 7.24 | 9.64 | 6.52 | 8.01 | 8.58 | 5.90 | 5.86 |
| Sm | 1.26 | 1.23 | 1.74 | 2.71 | 2.17 | 2.38 | 2.69 | 1.90 | 1.87 |
| Eu | 0.45 | 0.39 | 0.53 | 1.03 | 0.78 | 0.88 | 0.93 | 0.75 | 0.69 |
| Gd | 1.65 | 1.54 | 2.21 | 3.61 | 2.98 | 3.26 | 3.56 | 2.68 | 2.50 |
| Tb | 0.36 | 0.31 | 0.45 | 0.74 | 0.63 | 0.67 | 0.76 | 0.56 | 0.53 |
| Dy | 2.06 | 1.90 | 2.84 | 4.22 | 3.69 | 3.94 | 4.35 | 3.33 | 3.16 |
| Ho | 0.44 | 0.43 | 0.61 | 0.90 | 0.77 | 0.82 | 0.90 | 0.69 | 0.64 |
| Er | 1.43 | 1.31 | 1.99 | 2.56 | 2.18 | 2.36 | 2.59 | 1.99 | 1.82 |
| Tm | 0.24 | 0.23 | 0.33 | 0.47 | 0.41 | 0.42 | 0.48 | 0.37 | 0.35 |
| Yb | 1.79 | 1.61 | 2.44 | 2.87 | 2.54 | 2.72 | 3.20 | 2.46 | 2.23 |
| Lu | 0.31 | 0.27 | 0.40 | 0.38 | 0.32 | 0.36 | 0.41 | 0.32 | 0.29 |
| ΣLREE | 21.87 | 22.47 | 29.07 | 35.88 | 24.41 | 29.89 | 31.65 | 22.58 | 23.25 |
| ΣHREE | 8.26 | 7.59 | 11.26 | 15.75 | 13.52 | 14.56 | 16.25 | 12.40 | 11.51 |
| ΣREE | 30.13 | 30.06 | 40.33 | 51.63 | 37.93 | 44.45 | 47.90 | 34.98 | 34.76 |
| LREE/HREE | 2.65 | 2.96 | 2.58 | 2.28 | 1.81 | 2.05 | 1.95 | 1.82 | 2.02 |
| δEu _N | 0.95 | 0.86 | 0.82 | 1.01 | 0.94 | 0.96 | 0.92 | 1.01 | 0.97 |
| (La/Yb) _N | 1.59 | 1.81 | 1.59 | 1.57 | 1.25 | 1.42 | 1.25 | 1.24 | 1.45 |
| (Gd/Yb) _N | 0.75 | 0.77 | 0.73 | 1.02 | 0.94 | 0.97 | 0.90 | 0.88 | 0.91 |
| (La/Sm) _N | 2.10 | 2.21 | 2.08 | 1.55 | 1.36 | 1.51 | 1.39 | 1.49 | 1.61 |
| Cs | 3.32 | 1.40 | 1.99 | 0.00 | 0.00 | 0.00 | 0.00 | 0.00 | 0.00 |
| Rb | 8.30 | 9.70 | 19.90 | 2.60 | 2.30 | 4.50 | 4.30 | 2.90 | 3.30 |
| Sr | 242.90 | 118.90 | 149.80 | 169.37 | 161.60 | 210.74 | 211.37 | 152.15 | 143.54 |
| Ba | 134.55 | 119.36 | 140.34 | 27.00 | 21.20 | 33.10 | 42.50 | 28.90 | 24.90 |
| Ga | 0.00 | 0.00 | 0.00 | 0.00 | 0.00 | 0.00 | 0.00 | 0.00 | 0.00 |
| Nb | 1.50 | 1.65 | 1.56 | 0.87 | 0.80 | 1.15 | 1.15 | 0.61 | 0.84 |
| Ta | 0.21 | 0.21 | 0.22 | 0.08 | 0.08 | 0.14 | 0.09 | 0.07 | 0.10 |
| Zr | 51.80 | 73.40 | 62.10 | 72.88 | 51.60 | 70.34 | 69.90 | 47.52 | 52.15 |
| Hf | 2.67 | 3.63 | 3.36 | 5.66 | 4.25 | 5.87 | 5.86 | 3.89 | 4.18 |
| Th | 2.95 | 2.14 | 2.16 | 0.48 | 0.36 | 0.70 | 0.60 | 0.34 | 0.47 |
| V | 0.00 | 0.00 | 0.00 | 298.20 | 289.66 | 322.69 | 316.93 | 272.07 | 257.46 |
| Cr | 0.00 | 0.00 | 0.00 | 27.90 | 138.20 | 21.70 | 24.90 | 159.80 | 250.50 |
| Co | 0.00 | 0.00 | 0.00 | 17.92 | 28.83 | 22.90 | 20.67 | 24.16 | 28.62 |
| Sc | 0.00 | 0.00 | 0.00 | 28.89 | 43.75 | 39.04 | 38.27 | 35.88 | 38.24 |
| U | 0.43 | 0.44 | 0.52 | 0.00 | 0.00 | 0.00 | 0.00 | 0.00 | 0.00 |
| Y | 13.87 | 11.76 | 16.92 | 24.06 | 20.36 | 21.66 | 24.47 | 18.41 | 17.50 |

4 长石 U-Pb 年龄测定

斜长花岗岩样品破碎后分离出重砂, 经磁选和电磁选后, 在双目镜下挑出长石, 选取代表性长石, 制靶后通过透射光和反射光照相, 并在中国科学院地质与地球物理研究所采用阴极发光对长石结构进行了研究。在中国地质大学(北京)地学实验中心元素地球化学实验室对样品进行了 LA-ICP-MS 长石年代学的测试, 使用仪器为美国 New Wave 科技有

限公司的 UP 193 SS 型激光器, 激光波长为 193 nm, 载气为 He, 激光频率 10 Hz, 预剥蚀时间为 5 s, 剥蚀时间 45 s。质谱仪为美国 Agilent 科技有限公司的 7500a 型质谱仪, U、Th、Pb 等元素的积分时间为 20 ms, 普通铅校正依据 Andersen(2002)。样品长石的粒径较小(图 6), 约 40~60 μm, 为长柱状晶体, 无残留老核及变质边, 晶型较好, 发育有条带结构。长石的 U-Pb 同位素分析结果(表 2)显示, Th/U=0.32~1.38, 均大于 0.1, 属岩浆成因长石(Claesson *et al.*, 2000)。这与根据长石晶体生长特征判断的结

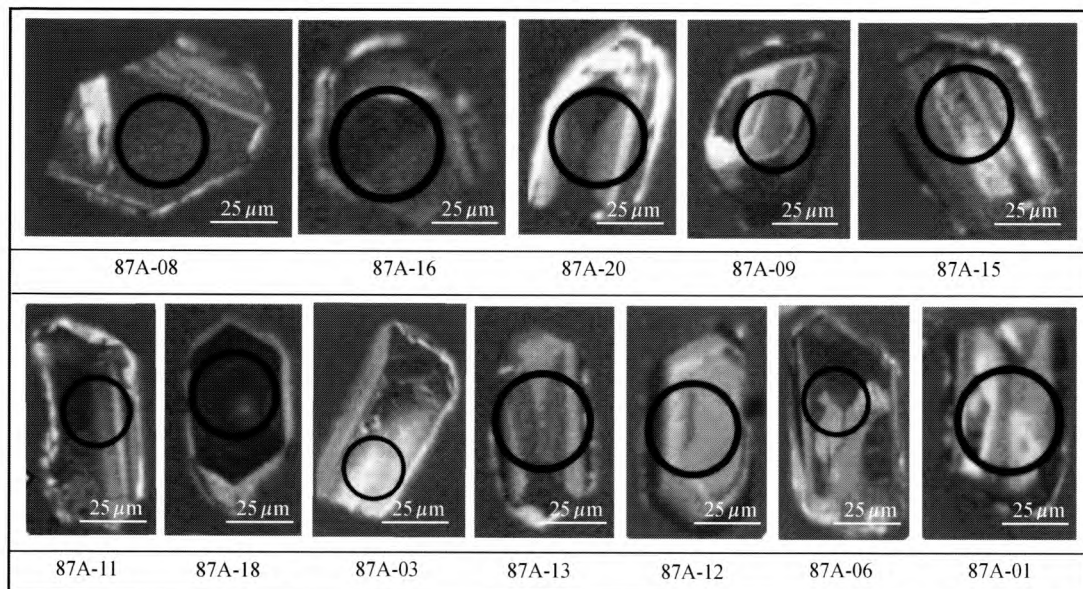


图 6 斜长花岗岩长石阴极发光图像(圈和数字分别表示 U-Pb 测试位置、测试编号)

Fig. 6 Cathodoluminescence image of the zircon from plagiogranite (the circle and the numeral represents the test location and serial number, respectively)

表 2 斜长花岗岩长石测年数据表
Table 2 Dating data of zircons from plagiogranite

| 点号 | $w_B/10^{-6}$ | | Th/U | 同位素比值 | | | | | | 年龄/Ma | | | | | |
|--------|------------------|-------------------|------|-----------------------------------|-----------|----------------------------------|-----------|----------------------------------|-----------|-----------------------------------|----------------------------------|----------------------------------|---|-----|-----|
| | ^{238}U | ^{232}Th | | $^{207}\text{Pb}/^{206}\text{Pb}$ | 1σ | $^{207}\text{Pb}/^{235}\text{U}$ | 1σ | $^{206}\text{Pb}/^{238}\text{U}$ | 1σ | $^{207}\text{Pb}/^{206}\text{Pb}$ | $^{207}\text{Pb}/^{235}\text{U}$ | $^{206}\text{Pb}/^{238}\text{U}$ | | | |
| 87A-01 | 549.08 | 251.08 | 0.46 | 0.04853 | 0.00192 | 0.19707 | 0.00761 | 0.02944 | 0.00028 | 125 | 72 | 183 | 6 | 187 | 3.5 |
| 87A-03 | 1261.79 | 1310.55 | 1.04 | 0.05090 | 0.00171 | 0.21833 | 0.00714 | 0.03110 | 0.00027 | 236 | 59 | 201 | 6 | 197 | 3.5 |
| 87A-06 | 504.59 | 284.53 | 0.56 | 0.05077 | 0.00196 | 0.21531 | 0.00811 | 0.03075 | 0.00029 | 230 | 70 | 198 | 7 | 195 | 3.5 |
| 87A-08 | 954.83 | 1317.82 | 1.38 | 0.05245 | 0.00190 | 0.21244 | 0.00751 | 0.02937 | 0.00027 | 305 | 64 | 196 | 6 | 187 | 3.5 |
| 87A-09 | 355.94 | 216.58 | 0.61 | 0.04891 | 0.00215 | 0.19904 | 0.00854 | 0.02951 | 0.00030 | 144 | 80 | 184 | 7 | 187 | 3.5 |
| 87A-11 | 1058.77 | 388.63 | 0.37 | 0.05252 | 0.00181 | 0.21744 | 0.00729 | 0.03002 | 0.00027 | 308 | 60 | 200 | 6 | 191 | 3.5 |
| 87A-12 | 452.42 | 266.64 | 0.59 | 0.04821 | 0.00198 | 0.20014 | 0.00801 | 0.03010 | 0.00030 | 110 | 73 | 185 | 7 | 191 | 3.5 |
| 87A-13 | 343.62 | 201.63 | 0.59 | 0.05252 | 0.00233 | 0.21438 | 0.00927 | 0.02960 | 0.00031 | 308 | 80 | 197 | 8 | 188 | 3.5 |
| 87A-14 | 592.74 | 572.98 | 0.97 | 0.04886 | 0.00199 | 0.20076 | 0.00798 | 0.02980 | 0.00030 | 141 | 74 | 186 | 7 | 189 | 3.5 |
| 87A-15 | 461.34 | 192.22 | 0.42 | 0.05010 | 0.00233 | 0.20491 | 0.00929 | 0.02966 | 0.00033 | 200 | 85 | 189 | 8 | 188 | 3.5 |
| 87A-16 | 633.77 | 539.14 | 0.85 | 0.04927 | 0.00222 | 0.20050 | 0.00883 | 0.02951 | 0.00032 | 161 | 82 | 186 | 7 | 187 | 3.5 |
| 87A-18 | 284.61 | 152.17 | 0.53 | 0.04799 | 0.00228 | 0.19989 | 0.00930 | 0.03020 | 0.00032 | 99 | 85 | 185 | 8 | 192 | 3.5 |
| 87A-20 | 765.68 | 245.03 | 0.32 | 0.05037 | 0.00180 | 0.20641 | 0.00719 | 0.02972 | 0.00027 | 212 | 64 | 191 | 6 | 189 | 3.5 |

注:同位素比值和年龄误差均为 1σ 。

果一致,说明锆石的结晶年龄可以代表斜长花岗岩的成岩时间。12颗锆石的13个测点在锆石U-Pb年龄谱和图(图7)中均位于 $^{206}\text{Pb}/^{238}\text{U}$ 与 $^{207}\text{Pb}/^{235}\text{U}$ 谐和线上或附近,说明锆石U-Pb年龄在误差范围内是谐和的,获得的 $^{206}\text{Pb}/^{238}\text{U}$ 加权平均年龄为 $189.8 \pm 1.9 \text{ Ma}$, MSWD=0.86。

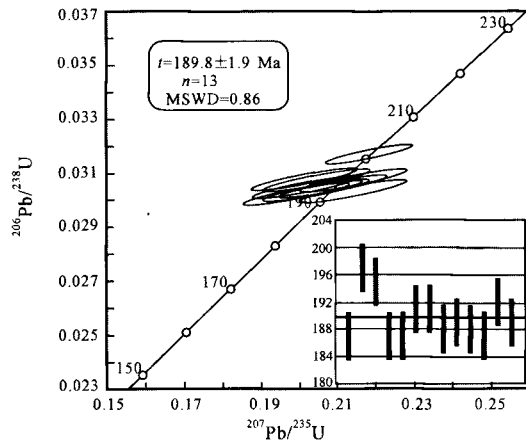


图7 斜长花岗岩锆石U-Pb年龄谱和图

Fig. 7 U-Pb concordia diagram of zircons from plagiogranite

5 讨论

5.1 斜长花岗岩的岩石成因

蛇绿岩中的花岗质岩石可以形成于蛇绿岩的不同阶段,成因也不同。传统意义上的斜长花岗岩是蛇绿岩代表的古大洋在洋底扩张形成洋壳时,由玄武质岩浆直接结晶分异形成的(David *et al.*, 1981)。后续研究表明,斜长花岗岩也可以在洋壳运动过程中由其内部发育的高温剪切带中岩石部分熔融形成(Pedersen & Malpas, 1984; Flagler & Spray, 1991);还可以在洋壳俯冲时由洋壳(包括大洋或海沟沉积物)部分熔融形成(Whitehead *et al.*, 2000)。

实验岩石学的模拟实验表明,蛇绿岩中的玄武质岩石和斜长花岗岩的元素La和Yb与SiO₂变异关系可以作为判别斜长花岗岩是分离结晶还是部分熔融形成的依据(Brophy, 2009)。如果斜长花岗岩由玄武质岩石部分熔融形成的岩浆结晶而成,那么斜长花岗岩中的元素La和Yb与玄武质岩石中的含量接近,也就是说随着SiO₂含量的增加,La和Yb的含量会保持不变;如果斜长花岗岩是由大洋中脊玄武质岩浆经过分离结晶形成,那么随着结晶分离作用的进行,残余岩浆中的元素La和Yb会逐渐升

高,即随着SiO₂含量的增加La和Yb的含量会逐渐升高(Brophy, 2009)。图8总结了不同成因的斜长花岗岩中La、Yb与SiO₂含量的关系。改则斜长花岗岩的La和Yb含量较低,与本区的中基性岩,如辉长岩、玄武岩及玄武安山岩接近,La和Yb含量并没有随SiO₂含量升高而变化,故推测斜长花岗岩是中基性岩经部分熔融作用形成的。

改则斜长花岗岩Al₂O₃含量小于15%,约为11.9%~13.2%,Na₂O/K₂O变化范围为3.64~8.23,Mg[#]变化范围为37~52,均值为42,具轻微的LREE富集。一般认为具有这种地球化学特点的斜长花岗岩形成于洋壳下部的高温剪切带中,由于板块运动使得洋壳下部热的、塑性的辉长岩发生低角度的剪切变形,同时水的加入降低辉长质岩石的熔点,在剪切热和辉长岩本身热的共同作用下,辉长质岩石先发生角闪岩相的变质作用,继而部分熔融,形成斜长花岗岩,在时间上,它略晚于蛇绿岩形成,它们的年龄代表了洋壳俯冲消减的时间(Pedersen and Malpas, 1984; 张玉修等, 2007)。这类斜长花岗岩常呈脉状产于蛇绿岩套中,与加拿大阿拉契亚Fournier蛇绿岩和挪威西部Karmoy蛇绿岩中的斜长花岗岩相似。

5.2 斜长花岗岩形成的构造背景

关于班公湖-怒江缝合带蛇绿岩形成的构造背景的认识并不一致,目前主要存在以下3种观点:①形成于洋中脊扩张的构造环境中(冯晔等, 2005; 曹圣华等, 2005),在晚三叠世早期-早侏罗世早期形成班公湖蛇绿岩(冯晔等, 2005);②形成于俯冲带上,如班公湖地区蛇绿岩形成于弧后盆地(王希斌等, 1987),在该带东段丁青和西段班公湖地区相继发现的玻安岩,以及与之共生的岛弧拉斑玄武岩和钙碱性玄武岩的存在,指示它形成于岛弧环境(张旗等, 1985; 史仁灯等, 2004);③本区不仅存在形成于俯冲带的SSZ型蛇绿岩,而且存在与现代大洋岩石圈在岩石学和地球化学特征上类似的地幔橄榄岩和上部熔岩,指示该区还存在MOR型蛇绿岩(史仁灯等, 2005; Shi *et al.*, 2008)。

改则地区蛇绿岩的成因构造背景存在同样的争论。林文第等(1990)认为改则蛇绿岩代表的是改则-色哇带的侏罗纪小洋盆的残留,是洋脊扩张的产物,而王保弟等(2007)认为改则拉果错蛇绿岩可能形成于弧间盆地环境,是由消减板片流体交代的地幔楔源区的部分熔融形成的,属于SSZ型蛇绿岩。

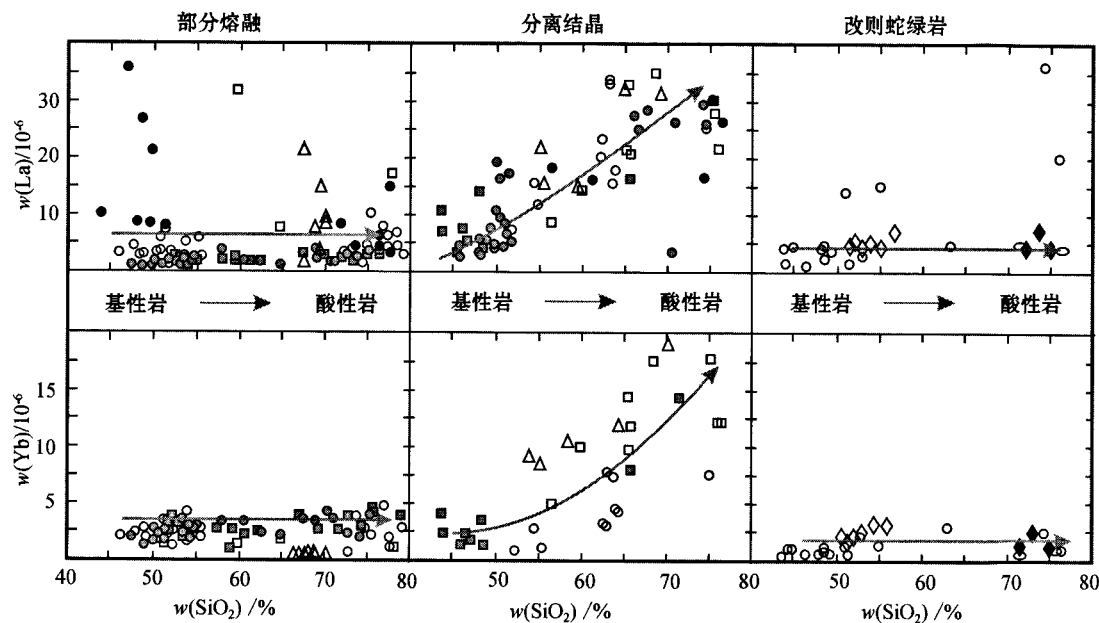


图 8 改则斜长花岗岩成因判别图解

Fig. 8 La - SiO₂ and Yb - SiO₂ diagram of Gaize plagiogranite

数据来源：部分熔融模型中，正方形：Flagler 和 Spray(1991)；空心圆：Malpas(1979), Jenner 等(1991)；实心正方形：Gerlach 等(1981)；浅色实心圆：Gillis & Coogen(2002)；深色实心圆：Pederson & Malpas(1984), Malpas(1979)；三角形：Kuibida 等(2009)；分离结晶模型中，正方形：Borsi 等(1996)；空心圆：Malpas(1979), Casey 等(1985), Siroky 等(1985)；实心正方形：Beccaluva 等(1999)；浅色实心圆：Saunders 等(1979)；深色实心圆：Pederson & Malpas(1984), Furnes 等(1980)；三角形：Heiko 等(1987)；改则蛇绿岩中，实心菱形：斜长花岗岩；空心菱形：玄武岩；椭圆：张玉修等(2007)；空心圆：西藏地质调查院^①

Data sources: Partial melting model: Square: Flagler & Spray(1991); Circle: Malpas(1979), Jenner et al. (1991); Solid square: Gerlach et al. (1981); Light-colored solid circle: Gillis & Coogen(2002); Dark solid circle: Pederson et al. (1984), Malpas(1979); Triangle: Kuibida et al. (2009); Fractional crystallization model: Square: Borsi(1996); Circle: Malpas(1979), Casey et al. (1985), Siroky et al. (1985); Solid square: Beccaluva et al. (1999); Light-colored solid circle: Saunders et al. (1979); Dark solid circle: Pederson et al. (1984), Furnes et al. (1980); Triangle: Heiko et al. (1987); Rhombus: Gaize plagiogranite; Solid rhombus: basalt; Ellipse: Zhang et al. (2007); Circle: Geological Survey of Tibet Autonomous Region^①

张玉修等(2007)认为改则附近拉果错蛇绿岩中斜长花岗岩是侏罗纪洋盆扩张的产物。本文研究表明，与改则斜长花岗岩伴生的熔岩在 TiO₂ - Mn - P₂O₅ 图解(图 9)上，均落在岛弧拉斑玄武岩区域内，并且斜长花岗岩与伴生熔岩的微量元素也显示岛弧火山岩的特点，推测改则蛇绿岩可能形成于俯冲带上的构造环境，属 SSZ 型蛇绿岩。

5.3 构造意义

班公湖-怒江带特提斯洋的存续时间一直存在争议。根据中国地质调查局最新 1:25 万地质填图表明，班公湖-怒江带是三叠纪-侏罗纪的洋盆(任纪舜等, 2004)，这与 Suess(1893)的特提斯洋定义以及 Sengör(1987)研究结果一致。但是已有的蛇绿岩上部熔岩同位素年代学以及放射虫时代资料均显示本区存在最老的形成于侏罗纪的洋盆(郭铁鹰等,

1991; 邱瑞照等, 2004; 张玉修等, 2007)，缺少三叠纪蛇绿岩的证据。这与特提斯构造带早期研究遇到的困难一样，即没有老的蛇绿岩或大陆边缘裂谷证据证明存在三叠纪的特提斯洋，这种现象被称为“特提斯之谜”(Tethyan Paradox)。前人对此提出过不少研究方案并做过大量的研究工作，但是始终未能从蛇绿岩角度找到解决这一问题的好办法(Sengör, 1987)。随着研究工作的不断深入，依据成因构造背景，将蛇绿岩分为了 MOR 型和 SSZ 型，前者形成于大洋扩张脊(Mid-ocean ridge)，后者形成于俯冲带上(Supra-Subduction Zone) (Pearce et al., 1984; Pearce, 2003)。目前统计结果表明，蛇绿岩在缝合带中易于保存，并且保存较好的绝大多数都属 SSZ 型(Stern, 2004)。班公湖-怒江带蛇绿岩的产出特点与世界上其他地区一样，保存下来的大多数是

^① 西藏自治区地质调查院. 2002. 中华人民共和国区域地质调查报告改则幅.

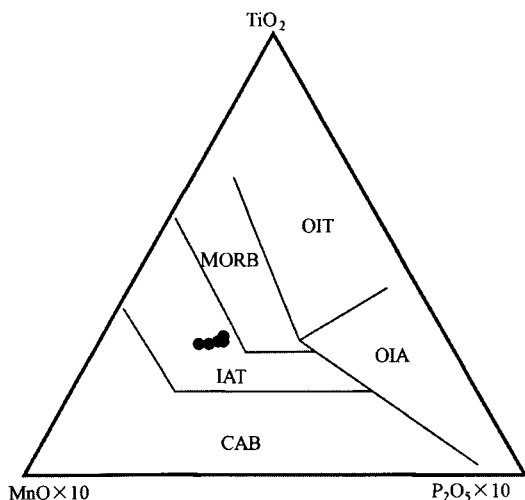


图9 改则蛇绿岩的熔岩 TiO_2 - Mn - P_2O_5 图解
(底图据 Mullen, 1983)

Fig. 9 TiO_2 - Mn - P_2O_5 discrimination diagram

of lavas from Gaize ophiolite (after Mullen, 1983)
MORB—洋脊玄武岩; OIT—洋岛拉斑玄武岩; OIA—洋岛碱性
玄武岩; IAT—岛弧拉斑玄武岩; CAB—钙碱性玄武岩
MORB—mid-ocean ridge basalt; OIT—oceanic island tholeiite;
OIA—oceanic island alkaline basalt; IAT—island-arc tholeiite;
CAB—calccalcic basalt

SSZ型蛇绿岩,因而用于定年的对象基本都是形成于俯冲带构造环境之上的SSZ型蛇绿岩,测得的年龄应该代表特提斯洋俯冲消减的时间而非扩张时间。例如,该缝合带西段的班公湖SSZ型蛇绿岩的同位素年龄为 167 ± 1.4 Ma,指示特提斯洋在中侏罗世由扩张开始向俯冲消减转换(史仁灯,2007)。这一理论模型可以帮助我们理解“特提斯之谜”。

班公湖-怒江带中东段东巧蛇绿岩铬铁矿中富Os合金的Re亏损年龄为 $207 \sim 276$ Ma(平均 238 ± 7 Ma, Shi et al., 2006)。虽然它是Re-Os同位素的模式年龄,但是与前人认为特提斯洋从三叠纪开始就已经打开的研究结果(Suess, 1893; Sengör, 1987; 王建平等,2002; 王冠民等,2002; 任纪舜等,2004)相符。也就是说,本区羌塘块体在这一时间已经从冈瓦纳大陆北缘裂解开来,所以可以用这一年龄作为班公湖-怒江带特提斯洋裂解的时间(Shi et al., 2008)。由于改则蛇绿岩与东巧蛇绿岩同处于班公湖-怒江缝合带,所以推测改则地区的特提斯洋存在晚二叠世-早三叠世的扩张作用(图10a)。

已有资料表明,班公湖-怒江带特提斯洋俯冲消减的时间在不同地段并不一样。蒋光武等(2009)和强巴扎西等(2009)综合沉积-构造演化、火山活动、侵入岩浆岩带、高压变质带和双变质带及堆晶辉长

岩等地质年代学的研究成果,认为最东段丁青地区俯冲消减时间为晚三叠世(图10b)。如前文所述,改则蛇绿岩中斜长花岗岩锆石U-Pb加权平均年龄为 189.8 ± 1.9 Ma,该年龄代表特提斯洋的俯冲消减时间,指示班公湖-怒江带特提斯洋在改则地区于早侏罗世发生了俯冲作用(图10c)。丁青以西、改则以东的东巧地区特提斯洋至少也在早侏罗世开始了俯冲消减(胡承祖,1990)。而在该带最西段班公湖地区,班公湖-怒江带特提斯洋至少从中侏罗世开始俯冲消减(史仁灯,2007)(图10d)。可见,班公湖-怒江带特提斯洋在东段的俯冲时间要早于西段,即在晚三叠世至中侏罗世期间,班公湖-怒江带特提斯洋自东段向西段依次发生俯冲消减,时间跨度约40~50 Ma。这种开始俯冲消减的顺序及时间跨度与班公湖-怒江带特提斯洋封闭的顺序和跨度是吻合的。王建平等(2002)研究表明,班公湖-怒江带特提斯洋东段的丁青蛇绿岩上被中侏罗世末至晚侏罗世滨浅海沉积地层不整合覆盖,表明此时洋盆已经闭合;在东巧地区,晚侏罗世-早白垩世东巧组、沙木罗组分别不整合于东巧蛇绿岩及木嘎岗日岩群之上,表明在东巧地区特提斯洋在晚侏罗世-早白垩世已经关闭;再向西至日土班公湖地区,大洋沉积可以延续到晚侏罗世(潘桂棠等,1997; Wang et al., 2000),在蛇绿岩之上不整合覆盖一套晚白垩世竟柱山组陆相沉积砂岩、砾岩,表明在西段特提斯洋至少在晚白垩世已经彻底封闭。王建平等(2002)认为,在西段日土班公湖地区,特提斯洋可能在晚侏罗世至早白垩世就已经关闭,郭铁鹰等(1991)根据蛇绿岩上覆地层上侏罗统推测班公湖地区新特提斯洋于早白垩世关闭。至此,班公湖-怒江缝合带彻底形成(图10e)。从该缝合带由东到西盖层沉积时代的对比可以看出,班公湖-怒江缝合带关闭时间由东向西逐渐变新,由东部的早侏罗世末到西部的晚侏罗世末,时代跨度约为40 Ma(王建平等,2002)。

6 结论

改则斜长花岗岩是在班公湖-怒江带特提斯洋板块俯冲过程中由中基性岩石部分熔融形成的,是改则蛇绿岩的组成部分。斜长花岗岩及伴生熔岩的微量元素具有岛弧火山岩的特点,指示改则蛇绿岩为SSZ型蛇绿岩。斜长花岗岩锆石的加权平均年龄为 189.8 ± 1.9 Ma,表明班公湖-怒江缝合带改则地区在

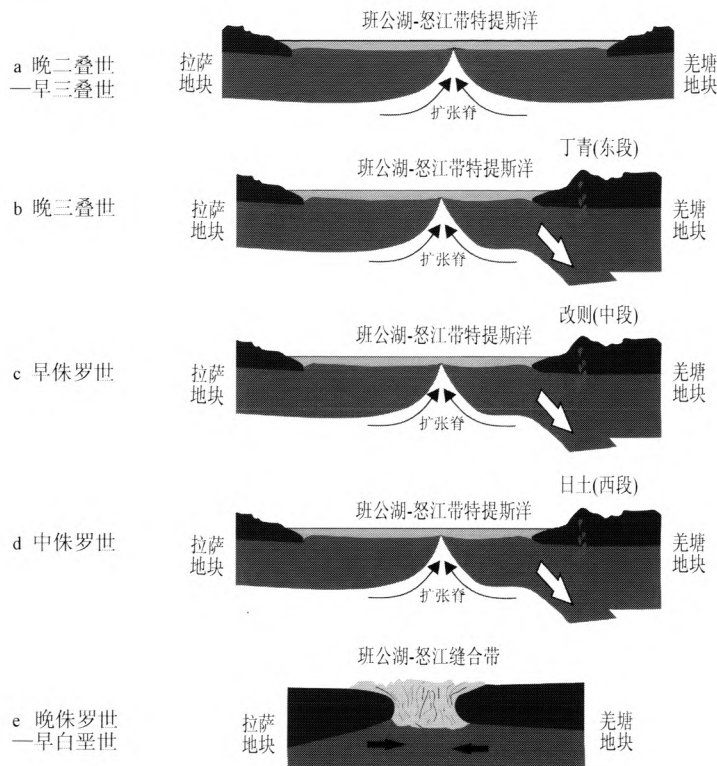


图 10 班公湖-怒江缝合带构造演化示意图

Fig. 10 Sketch map showing tectonic evolution of the Bangong-Nujiang suture (BNS)

a—根据 Re 亏损年龄 $t_{RD}=238 \pm 7$ Ma (Shi *et al.*, 2006, 2008) 及前人研究成果(Suess, 1893; Sengör, 1987; 王建平等, 2002; 王冠民等, 2002; 任纪舜等, 2004), 推测班公湖-怒江带特提斯洋在晚二叠世-早三叠世扩张裂解; b—在东段丁青地区, 班公湖-怒江带特提斯洋在晚三叠世发生俯冲消减(蒋光武等, 2009; 强巴扎西等, 2009); c—在中段改则地区, 班公湖-怒江带特提斯洋在早侏罗世(189.8 ± 1.9 Ma)发生俯冲消减, 同时在东巧地区也发生俯冲消减(胡承祖, 1990); d—在西段日土班公湖地区, 班公湖-怒江带特提斯洋在中侏罗世发生俯冲消减 (Shi, 2007); e—在晚侏罗世-早白垩世, 形成班公湖-怒江缝合带

a—Re depleted model age (t_{RD}) = 238 ± 7 Ma of Dongqiao ophiolite (Shi *et al.*, 2006, 2007) and previous work (Suess, 1893; Sengör, 1987; Wang *et al.*, 2002; Wang *et al.*, 2002; Ren and Xiao, 2004), suggesting that the Bangong-Nujiang Tethys Ocean was opened at least from late Permian-early Triassic; b—in Dingqing area, eastern part of the Bangong-Nujiang suture, the subduction of the Bangong-Nujiang Tethys Ocean took place in late Triassic (Jiang *et al.*, 2009; Qiangbazhaxi *et al.*, 2009); c—in Gaize area, middle part of the Bangong-Nujiang suture, the subduction of the Bangong-Nujiang Tethys Ocean took place in early Jurassic (189.8 ± 1.9 Ma); Meanwhile, subduction happened in Dongqiao area, middle part of the Bangong-Nujiang suture (Hu, 1990); d—in Bangong area of Ritu County, western part of the Bangong-Nujiang suture, subduction of the Bangong -Nujiang Tethys Ocean started before Middle Jurassic (Shi, 2007); e—during the late Jurassic and early Cretaceous period, the Bangong-Nujiang suture was formed completely

早侏罗世发生了俯冲作用, 早于该带西段班公湖地区, 晚于东段丁青地区特提斯洋俯冲, 即在晚三叠世至早侏罗世期间, 班公湖-怒江特提斯洋自东段向西段先后发生了俯冲消减作用。

致谢 张旗研究员对本文提出了建设性的修改意见, 钷石年龄测定得到了中国地质大学苏黎老师的帮助, 在此一并表示衷心感谢。

References

Andersen T. 2002. Correction of common lead in U-Pb analyses that do

- not report ^{204}Pb [J]. Chemical Geology, 192: 59~79.
Beccaluva L, Chinchilla-Chaves A L, Coltorti M, *et al.* 1999. Petrological and structural significance of the Santa Elena-Nicoya ophiolitic complex in Costa Rica and geodynamic implications[J]. Eur. J. Min., 11: 1 091~1 107.
Borsi L, Schärer U, Gaggero L, *et al.* 1996. Age, origin and Geodynamic significance of plagiogranites in Iherzolites and Gabbros of the Piedmont-Ligurian ocean basin[J]. Earth Planet Sci. Lett., 140: 227~241.
Boynton W V. 1984. Geochemistry of the rare earth elements: meteorite studies [A]. Henderson P. Rare Earth Element Geochemistry [C]. Elsevier, 63~114.
Brophy J G. 2009. La-SiO₂ and Yb-SiO₂ systematics in mid-ocean ridge magmas: implications for the origin of oceanic plagiogranite[J].

- Contrib. Mineral. Petrol., 158: 99~111.
- Cao Shenghua, Liao Liugen, Deng Shiquan, et al. 2005. Sequences, geochemistry and genesis of the Bangong Lake ophiolites in Xizang [J]. Sedimentary Geology and Tethyan Geology, 25(3): 101~110(in Chinese).
- Casey J F, Elthon D L, Siroky F S, et al. 1985. Geochemical and geological evidence bearing on the origin of the Bay of Island sand coastal complex ophiolites of western Newfoundland[J]. Tectonophysics, 116: 1~40.
- Claesson S V, Vertin and Bayanova H D. 2000. U-Pb zircon ages from a Devonian carbonatite dyke, Kola peninsula, Russia: a record of geological evolution from the Archaean to the Palaeozoic[J]. Lithos, 51: 95~108.
- Coleman R G and Peterman Z E. 1975. Oceanic plagiogranite[J]. J. Geophys. R., 80: 1 099~1 108.
- David C G, William P L and Hans G A L. 1981. Petrology and geochemistry of plagiogranite in the Canyon Mountain ophiolite, Oregon[J]. Contrib. Mineral. Petrol., 77: 82~89.
- Feng Ye, Liao Liugen and Xu Ping. 2005. The geological characteristics and the forming time of ophiolites in the region of the Bangong Lake, Tibet[J]. Volcanology & Mineral Resources, 26(3): 185~192(in Chinese).
- Flagler P A and Spray J G. 1991. Generation of plagiogranite by amphibolite anatexis in oceanic shear zones[J]. Geology, 19(1): 70~73.
- Furnes H, Sturt B A and Griffin W L. 1980. Trace element geochemistry of meta basalts from the Karmoy ophiolite, southwest Norwegian Caledonides[J]. Earth Planet. Sci. Lett., 50: 75~91.
- Gerlach D C, AveLallement H G and Leeman W P. 1981. An island arc Origin for the Canyon Mountain ophiolite complex, Eastern Oregon, USA[J]. Earth Planet Sci. Lett., 53: 255~265.
- Gillis K and Coogan L A. 2002. Anatetic migmatites from the roof of an Ocean ridge magma chamber [J]. J. Petrol., 43: 2 075~2 095.
- Guo Tieying, Liang Dingyi, Zhang Yizhi, et al. 1991. Ali Geology in Tibet[M]. Beijing: Geological Publishing House, 201~204 (in Chinese).
- Heiko G H, Wildberg and Karlsruhe. 1987. High level and low level plagiogranites from the Nicoya ophiolite complex, Costa Rica, Central America[J]. Geologische Rundschau, 76: 285~301.
- Hu Chengzu. 1990. Characteristics of shiquanhe-guchang ophiolite belt and its geologic significance[J]. Journal of Chengdu University of Technology (Science & Technology Edition), 17(1): 23~30 (in Chinese).
- Jenner G A, Dunning G R, Malpas J, et al. 1991. Bay of Island sand little Port complexes revisited: age, geochemical and isotopic evidence con? rm suprasubduction-zone origin [J]. Can. J. Earth Sci., 28: 1 635~1 652.
- Jiang Guangwu, Xie Yaowu, Bai Zhenping, et al. 2009. Tectonic evolution of Dingqing-Bitu segment of Bangonghu-Nujiang suture zone in Qinghai-Tibet Plateau, China[J]. Geological Bulletin of China, 28(9): 1 260~1 267 (in Chinese).
- Kuibida M L, Kruk N N, Vladimirov A G, et al. 2009. U-Pb isotopic age, composition, and sources of the plagiogranites of the Kalba Range, Eastern Kazakhstan[J]. Geochemistry, 424: 72~76.
- Le Maître R W, Bateman P, Dudek A, et al. 1989. A classification of Igneous and Glossary of Terms[M]. Oxford: Blackwell.
- Lin Wendi and Chen Dequan. 1990. The feature of the ophiolite in Grze-Sewa, north Xizang[J]. Journal of Chengdu University of Technology (Science & Technology Edition), 17(2): 16~24 (in Chinese).
- Malpas. 1979. Two contrasting trondhjemite associations from transported ophiolites in Western Newfoundland: initial report [A]. Barker. Trondhjemites, Dacites and Related Rocks[C]. Elsevier, Amsterdam, 465~487.
- Mullen E D. 1983. MnO/TiO₂/P₂O₅: a minor element discriminant for basaltic rocks of oceanic environments and its implications for petrogenesis[J]. Earth Planet. Sci. Lett., 62: 53~62.
- Pan Guitung, Chen Zhiliang, Li Xingzhen, et al. 1997. Tectonic Evolution of Eastern Tethyan Geology[M]. Beijing: Geological Publishing House, 218 (in Chinese).
- Pearce J A. 2003. Supra-subduction zone ophiolites: the search for modern analogues[A]. Dilek & Newcomb. Ophiolite Concept and the Evolution of Geological Thought[C]. Colorado: Geological Society of American Special Paper, 373: 269~293.
- Pearce J A, Lippard S J and Roberts S. 1984. Characteristics and tectonic significance of supra-subduction zone ophiolites[A]. Kokelaa and Howells. Marginal Basin Geology[C]. Geological Society of London Special Publication 16. London: Blackwell Scientific Publications, 77~94.
- Pedersen R B and Malpas J. 1984. The origin of oceanic plagiogranites from the Karmoy ophiolite, western Norway[J]. Contrib. Mineral. Petrol., 88: 36~52.
- Qiangba Zhai, Xie Yaowu, Wu Yanwang, et al. 2009. Zircon SIMS U-Pb dating and its significance of cumulate gabbro from Dêngqên ophiolite, eastern Tibet, China[J]. Geological Bulletin of China, 28(9): 1 253~1 258 (in Chinese).
- Qiu Ruizhao, Zhou Su, Deng Jinfu, et al. 2004. Dating of gabbro in the Shemalagou ophiolite in the western segment of the Bangong Co-Nujiang ophiolite belt, Tibet-with a discussion of the age of the Bangong Co-Nujiang ophiolite belt[J]. Chinese Geology, 31(3): 262~268 (in Chinese).
- Ren Jishun and Xiao Liwei. 2004. Lifting the mysterious veil of the tectonics of the Qinghai-Tibet Plateau by 1:250000 geological mapping [J]. Geological Bulletin of China, 23(1): 1~11 (in Chinese).
- Saunders A D, Tarney J, Stern C R, et al. 1979. Geochemistry of Mesozoic marginal basin floor igneous rocks from southern Chile [J]. Part I. Geol. Soc. Am. Bull., 90: 237~258.
- Sengör A M C. 1987. Tectonics of the Tethysides: Orogenic collage development in a collisional setting[J]. Ann. Rev. Earth Planet. Sci., 15: 213~244.
- Shi Rendeng. 2007. Age of Bangong Lake SSZ ophiolite constraints the time of the Bangong Lake – Nujiang Neo-Tethys[J]. Chinese Sci. Bull., 52(7): 936~941.
- Shi Rendeng, Yang Jingsui and Xu Zhiqin. 2008. The Bangong Lake ophiolite (NW Tibet) and its bearing on the tectonic evolution of the Bangong-Nujiang suture zone[J]. J. Asian Earth Sci., 32: 438~457.

- Shi Rendeng, Yang Jingsui, Xu Zhiqin, et al. 2004. Discovery of boninite series volcanic rocks in the Bangong Lake ophiolite mélange, Western Tibet and its tectonic implication [J]. Chinese Sci. Bull., 12: 1 272~1 278.
- Shi Rendeng, Yang Jingsui, Xu Zhiqin, et al. 2005. Recognition of MOR- and SSZ-type ophiolites in the Bangong Lake ophiolite mélange, western Tibet: evidence from two kinds of mantle peridotites[J]. Acta Petrologica et Mineralogica, 24(5): 397~408(in Chinese with English abstract).
- Shi Rendeng, Zhi Xiachen, Suzanne Y O'Reilly, et al. 2006. Multiple events in oceanic upper mantle: Re-Os-Ir alloys in Tibetan ophiolites [J]. Geochim. Cosmochim. Acta, 70(18-supplement 1), A583.
- Siroky F X, Elthon D L, Casey J F, et al. 1985. Major element variations in basalts and diabases from the North Arm Mountain Massif, Bay of Islands ophiolite: implications for magma chamber processes at mid-ocean ridges[J]. Tectonophysics, 116: 41~61.
- Sorenson S S and Grossman J N. 1989. Enrichment of trace elements in garnet amphibolites from a Paleo-subduction zone: Catalina Schist, southern California[J]. Geochim. Cosmochim. Acta, 53: 3 155~3 177.
- Stern R J. 2004. Subduction initiation: spontaneous and induced[J]. Earth Planet. Sci. Lett., 226: 275~292.
- Suess E. 1893. Are great ocean depths permanent? [J]. Nat. Sci., 2: 180~187.
- Thompson R N. 1982. Magmatism in the British Tertiary volcanic province, Scott [J]. J. Geol., 18: 49~107.
- Wang Baodi, Xu Jifeng, Zeng Qinggao, et al. 2007. Geochemistry and genesis of Lhaguo Tso ophiolite in south of gerze area, center Tibet [J]. Acta Petrologica Sinica, 23(6): 1 521~1 530(in Chinese).
- Wang Guanmin and Zhong Jianhua. 2002. Tectonic sedimentary evolution of the west segment of the Bangong Co-Nujiang Structure belt in the Triassic and Jurassic [J]. Geological Review, 48(3): 297~303(in Chinese).
- Wang Jianping. 2000. Geological features of the eastern sector of the Bangong Co-Nujiang River suture zone, Tethyan evolution[J]. Acta Geologica Sinica, 74(2): 229~235.
- Wang Jianping, Liu Yanming, Li Qusheng, et al. 2002. Stratigraphic division and geological significance of the Jurassic cover sediments in the eastern sector of the Bangong Lake-Dêngqên ophiolite belt in Tibet[J]. Geological Bulletin of China, 21(7): 405~410(in Chinese).
- Wang Xibin, Bao Peisheng, Deng Wanming, et al. 1987. Ophiolites of Tibet [M]. Beijing: Geological Publishing House, 1~124(in Chinese).
- Whitehead J, Dunning G R and Spray J G. 2000. U-Pb geochronology and origin of granitoid rocks in the Thetford Mines ophiolite, Canadian Appalachians[J]. Geol. Soc. Am. Bull., 112(6): 915~928.
- Zhang Kuanzhong and Chen Yulu. 2007. Plagiogranite in the Guchang ophiolites in Xizang[J]. Sedimentary Geology and Tethyan Geology, 27(1): 32~37(in Chinese).
- Zhang Qi and Yang Ruiying. 1986. The boninite-like pluton in ophiolite from Dêngqên, Xizang, and its geological significance[J]. Chinese Sci. Bull., 31(6): 405~408.
- Zhang Yuxiu, Zhang Kaijun, Li Bing, et al. 2007. Zircon SHRIMP U-Pb geochronology and petrogenesis of the plagiogranites from the Lagkor Lake ophiolite Gerze, Tibet, China[J]. Chinese Sci. Bull., 52(5): 651~659.
- ### 附中文参考文献
- 曹圣华, 廖六根, 邓世权, 等. 2005. 西藏班公湖蛇绿岩组合层序、地球化学及其成因研究[J]. 沉积与特提斯地质, 25(3): 101~110.
- 冯晔, 廖六根, 徐平. 2005. 西藏班公湖蛇绿岩地质特征及形成时代[J]. 资源调查与环境, 26(3): 185~192.
- 郭铁鹰, 梁定益, 张宜智, 等. 1991. 西藏阿里地质[M]. 北京: 地质出版社, 201~204.
- 胡承祖. 1990. 狮泉河-古昌-永珠蛇绿岩带特征及其地质意义[J]. 成都理工大学学报(自然科学版), 17(1): 23~30.
- 蒋光武, 谢尧武, 白珍平. 2009. 青藏高原班公湖-怒江缝合带丁青-碧土段大地构造演化[J]. 地质通报, 28(9): 1 260~1 267.
- 林文第, 陈德全. 1990. 哇地区的蛇绿岩特征[J]. 成都地质学院学报, 17(2): 16~24.
- 潘桂棠, 陈智梁, 李兴振, 等. 1997. 东特提斯地质构造形成演化[M]. 北京: 地质出版社, 218.
- 强巴扎西, 谢尧武, 吴彦旺, 等. 2009. 藏东丁青蛇绿岩中堆晶辉长岩锆石 SIMS U-Pb 定年及其意义[J]. 地质通报, 28(9): 1 253~1 258.
- 邱瑞照, 周肃, 邓晋福, 等. 2004. 西藏班公湖-怒江西段舍马拉沟蛇绿岩中辉长岩年龄测定——兼论班公湖-怒江蛇绿岩带形成时代[J]. 中国地质, 31(3): 262~268.
- 任纪舜, 肖黎薇. 2004. 1:25 万地质填图进一步揭开了青藏高原大地构造的神秘面纱[J]. 地质通报, 23(1): 1~11.
- 史仁灯. 2007. 班公湖 SSZ 型蛇绿岩年龄对班-怒洋时限的制约[J]. 科学通报, 52(2): 223~227.
- 史仁灯, 杨经绥, 许志琴, 等. 2004. 西藏班公湖蛇绿混杂岩中玻安岩系火山岩的发现及构造意义[J]. 科学通报, 49(12): 1 179~1 184.
- 史仁灯, 杨经绥, 许志琴, 等. 2005. 西藏班公湖存在 MOR 型和 SSZ 型蛇绿岩—来自两种不同地幔橄榄岩的证据[J]. 岩石矿物学杂志, 24(5): 397~408.
- 王保弟, 许继峰, 曾庆高, 等. 2007. 西藏改则地区拉果错蛇绿岩地球化学特征及成因[J]. 岩石学报, 23(6): 1 521~1 530.
- 王冠民, 钟建华. 2002. 班公湖-怒江构造带西段三叠纪-侏罗纪构造-沉积演化[J]. 地质论评, 48(3): 297~303.
- 王建平, 刘彦明, 李秋生, 等. 2002. 班公湖-丁青蛇绿岩带东段侏罗纪盖层沉积的地层划分[J]. 地质通报, 21(7): 405~410.
- 王希斌, 鲍佩声, 邓万明, 等. 1987. 西藏蛇绿岩[M]. 北京: 地质出版社, 1~124.
- 张宽忠, 陈玉禄. 2007. 古昌蛇绿岩中的斜长花岗岩特征[J]. 沉积与特提斯地质, 27(1): 32~37.
- 张旗, 杨瑞英. 1985. 西藏丁青蛇绿岩中玻镁安山岩类的深成岩及其地质意义[J]. 科学通报, 16: 1 243~1 245.
- 张玉修, 张开均, 黎兵, 等. 2007. 西藏改则南拉果错蛇绿岩中斜长花岗岩锆石 SHRIMP-U-Pb 年代学及其成因研究[J]. 科学通报, 52(1): 100~106.